SIR Meta Distribution of K-Tier Downlink Heterogeneous Cellular Networks with Cell Range Expansion

Yuanjie Wang, Martin Haenggi, *Fellow, IEEE*, and Zhenhui Tan, *Senior Member, IEEE*

***Abstract*—Heterogeneous cellular networks (HCNs) constitute a necessary step in the evolution of cellular networks. In this paper, we apply the signal-to-interference ratio (SIR) meta distribution framework for a refined SIR performance analysis of HCNs, focusing on K-tier heterogeneous cellular networks based on the homogeneous independent Poisson point process (HIP) model, with range expansion bias (offloading bias) in each tier. Expressions for the b-th moment of the conditional success probability for both the entire network and each tier are derived, based on which the exact meta distributions and the beta approximations are evaluated and compared. Key performance metrics including the mean success probability, the variance of the conditional success probability, the mean local delay and the asymptotic SIR gains of each tier are obtained. The results show that the biases are detrimental to the overall mean success probability of the whole network and that the b-th moment curve of the conditional success probability of each tier can be tightly approximated by the horizontal shifted versions of the first moment curve of the single-tier PPP network. We also provide lower bounds for the region of the active probabilities of the base stations to keep the mean local delay of each tier finite.**

***Index Terms*—Stochastic geometry, Poisson point process, heterogeneous cellular network, SIR, coverage, meta distribution, offloading.**

I. INTRODUCTION

A. Motivation

Heterogeneous cellular networks (HCNs), consisting of various types of base stations such as macro, pico and femto, are a necessary step in the evolution of cellular networks to meet the explosive demand in mobile data traffic growth and various emerging applications [1]. For seamless coverage, it is essential to understand the signal-to-interference ratio (SIR) distribution, especially at high deployment densities, which makes the network interference-limited. In the literature, the mathematical analysis for the SIR distribution in conventional single-tier cellular network and HCNs mainly relies on the application of Poisson point process (PPP) theory in stochastic geometry [2]–[10], which has been shown to be a powerful tool in recent years.

Yuanjie Wang is with the National Computer Network Emergency Response Technical Team/Coordination Center of China (CNCERT/CC), Beijing, 100029, China (e-mail: wang.yuanjie@outlook.com). Martin Haenggi is with the Dept. of Electrical Engineering, University of Notre Dame, IN, 46556, USA (e-mail: mhaenggi@nd.edu). Zhenhui Tan is with the State Key Laboratory of Railway Traffic Control and Safety, Beijing Jiaotong University, Beijing, 100044, China. The work was supported by National Natural Science Foundation of China (61471030, 61601018), National Science and Technology Major Project of China (2015ZX03001027-003) and the US National Science Foundation (grant CCF 1525904).

However, the conventional SIR analysis for the HCNs is restricted to the mean success probability $p_{\rm s}(\theta) \triangleq \mathbb{P}(\mathsf{SIR} > \theta)$, defined as the complementary cumulative distribution function (CCDF) of the SIR evaluated at the typical link. Such a performance metric is merely a macroscopic quantity by averaging the conditional success probability (link reliability) $P_{\rm s}(\theta) \triangleq \mathbb{P}(\mathsf{SIR} > \theta \mid \Phi)$ over the underlying point process Φ, hence it provides no information about the difference between links. In contrast, the network operators' concerns for the real deployment of HCNs are questions such as "How are the link reliabilities distributed among users in different tiers and/or in the whole network?", or "How will the offloading affect the SIR performance of different tiers?", or "What is the reliability level that the '5% user'[1] can achieve in each tier?"

To obtain such fine-grained information on the SIR performance, the meta distribution concept was introduced in [11], which characterizes the distribution of the conditional success probabilities of the individual links given the point process. The lack of study of the meta distribution for HCNs with offloading biasing among different tiers motivates our study in this paper. We shall see that the meta distribution of SIR is a framework that facilitates the analysis for a series of performance metrics including the variances of the link reliability, the mean local delay and the asymptotic gains for HCNs.

B. Related Work

For the SIR-related analysis based on stochastic geometry in HCNs, the most commonly used model is the homogeneous independent Poisson (HIP) model, where BSs of each tier follow a homogeneous independent Poisson point process [12, Def. 2]. [4] utilized the HIP model with the (biased) nearest-BS association and considered offloading between different tiers, where offloading was implemented by biasing the transmit power of different tiers. In [5], coordinated multipoint joint transmission (CoMP) in HCN was analyzed and it was shown, as a special case (namely no-CoMP), that the result for a single tier in [3] also holds for arbitrary tiers.

Instead of the (biased) nearest-BS association adopted in the above-mentioned works, there is also the line of work using the maximum instantaneous SINR association, such as [6]–[10]. [6] studied the coverage (success) probability and the average rate of the HIP model for the SINR thresholds greater

[1]The "5% user" refers to the user whose performance ranks at the 5th-percentile.

than 0 dB under both open and closed access. [7] utilized the HIP model and determined the coverage probability from the joint CCDF of the SINR at the typical user with the SINR thresholds extended to all regime. [8] and [9] extended the SINR threshold to less than 0 dB and established exact results for the maximum instantaneous SINR association rule with arbitrary shadowing in HCNs by the K-coverage probability. As for the fading model, it should be noted that different from [6], where only Rayleigh fading is considered, it has been shown that the same result applies to arbitrary fading in [10].

As for modeling the HCNs with more general point processes, [13] proposed two models for the two-tier HCN with the inter-tier independence modeled by combining the PPP and the Poisson hole process, and the intra-tier independence taken into account by combining the PPP and Matern cluster process respectively, yielding more accurate results for the outage probability and the area spectral efficiency. In [14], for HCNs consisting of general point processes as each tier with unbiased association, the authors studied the SIR distribution by using the shifted versions of the PPP SIR distributions as approximations.

Most of these above-discussed works related to the SIR analysis in HCNs only analyze the mean success probability without delving into the SIR performance at the individual link level. To overcome this limitation, we need to develop the meta distribution framework for the HCNs.

The meta distribution has been applied to different scenarios since it was formally formulated in [11], where the analysis of single-tier Poisson bipolar networks with ALOHA channel access and the downlink of Poisson cellular networks laid the foundation of the concept. It was applied to study D2D communication underlaid with the downlink of Poisson cellular networks [15], uplink and downlink Poisson cellular networks with fractional power control [16], D2D communications with interference cancellation [17], millimeter-wave D2D networks [18], the spatial outage capacity [19], and downlink coordinated multi-point transmission/reception (CoMP) in cellular networks [20]. These studies revealed some interesting new insights that are of significance to the deployment of real networks.

C. Contributions

In this paper, we develop an SIR meta distribution analysis framework for the HIP downlink model under Rayleigh fading. We show that this framework enables a comprehensive understanding of a series of key performance metrics and network design problems. Specifically,

- We derive exact analytical expressions of the b-th moment of the conditional success probability for both the overall typical user and the typical user in each tier.
- We show that the beta distribution is an excellent approximation for the exact meta distribution of both the entire network and each tier.
- We reveal that both the b-th moment and the variance of the conditional success probability for each tier can be efficiently approximated by horizontally shifting the mean success probability curve of the single-tier PPP according to the asymptotic SIR gains, whose expressions are given explicitly.
- We rigorously study the effects of the offloading biases on both the entire network and each tier in terms of the first moment and variance of the conditional success probability.
- We extend the model to include random base station activity by ALOHA and derive analytical expressions of the b-th moment of the conditional success probability for both the overall typical user and the typical user in each tier.
- We derive lower bounds of the region of ALOHA probabilities so that the mean local delay remains finite under the effect of random base station activity.

TABLE I
LIST OF SYMBOLS

Symbol	Definition
Φ_i	PPP to constitute the i-th tier
λ_i	Intensity of BSs in the i-th tier
P_i	Transmission power of the i-th tier
B_i	Range expansion bias of the i-th tier
Ψ	Point process to constitute the HCN
α	Path loss exponent
$\nu(o)$	Serving BS of the typical user at the origin
$\iota(\mathrm{x})$	Tier index of BS x
h	Small scale fading channel gain
θ	SIR threshold for success transmission
$P_{\mathrm{s}}(\theta)$	Conditional success probability
M_b	b-th moment of $P_{\mathrm{s}}(\theta)$
G_0	Asymptotic SIR gain at $\theta \to 0$
G_∞	Asymptotic SIR gain at $\theta \to \infty$
p_i	BS active probability for the i-th tier

D. Organization

The rest of the paper is organized as follows: Section II introduces the system model and the concept of the SIR meta distribution in HCNs. Section III develops the general framework for the analysis of HCNs using the meta distribution, wherein we derive exact analytical expressions of the b-th moment of the conditional success probability, both for the entire network and for each individual tier, and discuss various key performance metrics and some network design problems related to offloading. Section III-D extends the SIR meta distribution to the analysis of random base station activity. Section V concludes the paper.

Notations: The mean of the random variable X is denoted by $\mathbb{E}[X]$. The probability of event A is denoted by $\mathbb{P}(A)$. The Gaussian hypergeometric function is denoted by ${}_2F_1(.,.;.;.)$. The meanings of the main symbols employed in this paper is listed in Table I.

II. System Model

A. SIR Model

We consider a general K-tier heterogeneous cellular network model, where BSs of each tier follow a homogeneous independent Poisson point process Φ_i with intensity λ_i. This is the so-called homogeneous independent Poisson (HIP) model

[12, Def. 2]. For the BSs of the i-th tier, the transmit power is P_i, and the range expansion bias is B_i. For BS $\mathrm{x} \in \Psi = \bigcup_{i\in[K]} \Phi_i$, $\iota(\mathrm{x}) \in [K]$, denotes its tier number, and $[K] = \{1, 2, ...K\}$. We assume the standard power-law path loss model with exponent $\alpha > 2$, and define $\delta = 2/\alpha$. The downlink association rule is the biased nearest-BS association, *i.e.*, for the typical user at the origin o, its serving BS $\nu(o)$ is drawn from all BSs according to

$$\nu(o) = \arg\max_{\mathrm{x}\in\Psi}\{P_{\iota(\mathrm{x})}B_{\iota(\mathrm{x})}\|\mathrm{x}\|^{-\alpha}\}, \tag{1}$$

where $\iota(\mathrm{x})$ is the tier index of BS x.

The power fading coefficient associated with BS $\mathrm{x} \in \Psi$ is denoted by h_{x}, which is exponentially distributed with $\mathbb{E}(h_{\mathrm{x}}) = 1$ (Rayleigh fading). R_j is the distance from the typical user to the nearest BS in Φ_j. First we focus on the fully loaded case on a certain resource block (RB), *i.e.*, all BSs are always active on the RB in consideration.

Letting $\mathrm{x}_0 = \nu(o)$, for the typical user at the origin, the received signal-to-interference ratio (SIR) is given by

$$\mathsf{SIR}_o = \frac{P_{\iota(\mathrm{x}_0)}h_{\mathrm{x}_0}\|\mathrm{x}_0\|^{-\alpha}}{\sum\limits_{\mathrm{x}\in\Psi\setminus\{\mathrm{x}_0\}} P_{\iota(\mathrm{x})}h_{\mathrm{x}}\|\mathrm{x}\|^{-\alpha}}. \tag{2}$$

B. Meta Distribution and Fine-grained Information for HCNs

The SIR meta distribution for single-tier cellular networks is the two-parameter function defined as [11]

$$\bar{F}(\theta, t) \triangleq \bar{F}_{P_{\mathrm{s}}}(t) = \mathbb{P}(P_{\mathrm{s}}(\theta) > t), \quad \theta \in \mathbb{R}^+,\ t \in [0, 1], \tag{3}$$

which is the CCDF of the conditional success probability (link reliability) P_{s}. The b-th moment of the meta distribution is denoted by $M_b(\theta) \triangleq \mathbb{E}(P_{\mathrm{s}}(\theta)^b)$.

M_b is of great importance for the analysis of the network performance, since many relevant metrics are special cases, as explained in the following.

- M_1 is the standard success probability (or coverage probability) used in many stochastic geometry studies, it is the spatial average of all links in the point process.
- M_{-1} is usually called the mean local delay. To see this, let L denote the number of transmission attempts needed until a packet is successfully received (decoded) over a wireless link and assume that the fading over different transmission intervals is independent. Then given the point process, L is geometrically distributed with parameter P_{s}, *i.e.*, $\mathbb{P}(L = k \mid \Phi) = (1 - P_{\mathrm{s}})^{k-1}P_{\mathrm{s}}, \quad k \in \mathbb{N}$, then
$$\mathbb{E}[L] = \mathbb{E}[\mathbb{E}[L \mid \Phi]] = \mathbb{E}\left[\frac{1}{P_{\mathrm{s}}}\right] = M_{-1}.$$
- The variance $M_2 - M_1^2$ is a metric characterizing the concentration of the link reliabilities of the individual links in the network, hence it reflects the fairness among the users.

These metrics are particularly important information to the operators for the optimization of the networks.

In the context of HCNs, we consider two types of SIR meta distributions, one is for the overall network (*i.e.*, the overall typical user) and the other is specific to the i-th tier, obtained by conditioning on the typical user connecting to that tier. In the following, we use the label (i) for the quantities related to the i-th tier meta distributions.

III. SIR Meta Distribution Framework

In this section we derive the general analytical expression for the b-th moment of the meta distribution in the HIP model with biasing.

A. Moments of the Conditional Success Probability

First, we state a lemma about the conditional and average access probabilities for the typical user connecting to the given i-th tier, which is a slight reformulation of [4, Lemma 1]. Hence the proof is omitted.

Lemma 1 (Access probability) *Defining $\iota(\mathrm{x}_0) \triangleq \iota(\nu(\mathrm{o}))$, the conditional access probability for the typical user connecting to the i-th tier given R_i is*

$$\mathbb{P}(\iota(\mathrm{x}_0) = i \mid R_i) = \prod_{j\neq i} e^{-\lambda_j\pi(\hat{P}_{ij}\hat{B}_{ij})^{\delta}R_i^2}, \tag{4}$$

and the access probability that the typical user is associated with the i-th tier is

$$p_{\mathrm{a}}^{(i)} \triangleq \mathbb{P}(\iota(\mathrm{x}_0) = i) = \frac{1}{\sum\limits_{j\in[K]} \hat{\lambda}_{ij}(\hat{P}_{ij}\hat{B}_{ij})^{\delta}}, \tag{5}$$

where $\hat{\lambda}_{ij} = \lambda_j/\lambda_i$, $\hat{P}_{ij} = P_j/P_i$ and $\hat{B}_{ij} = B_j/B_i$.

Next we present the first main result on the moments of the conditional success probability.

Theorem 1 (Moments for the K-tier HCNs) *For the overall typical user in the K-tier HIP model with range expansion, the b-th moment of the conditional success probability is given by*

$$M_b = \sum_i \frac{1}{\sum\limits_j \hat{\lambda}_{ij}(\hat{P}_{ij}\hat{B}_{ij})^{\delta}\ {}_2F_1(b, -\delta; 1-\delta; -\theta\hat{B}_{ij}^{-1})}, \tag{6}$$

where $i,\ j \in [K]$, $\hat{\lambda}_{ij} = \lambda_j/\lambda_i$, $\hat{P}_{ij} = P_j/P_i$ and $\hat{B}_{ij} = B_j/B_i$.

Proof: See Appendix A. ∎

Corollary 1 (Moments without range expansion) *For the overall typical user, the b-th moment M_b with no range expansion in any tier,* i.e., *$B_i = 1$ for $i \in [K]$, is given by*

$$M_b = \frac{1}{{}_2F_1(b, -\delta; 1-\delta; -\theta)}, \quad b \in \mathbb{C}. \tag{7}$$

Proof: This can be easily obtained by setting $B_i = 1$ for $i \in [K]$ in (6). ∎

Remark 1 *The b-th moment of the meta distribution of the overall typical user in a HIP-based K-tier downlink HCN without range expansion in any tier is the same as that in a* *single-tier network [11, Thm. 2]. Hence the meta distribution is the same. This shows that the multi-tier architecture does not improve the performance of the 5% user (or, more generally, the fairness between the users).*

Corollary 2 (Moments for the typical user in the i-th tier) *Conditioned on the typical user connecting to the i-th tier, the b-th moment of the meta distribution is given by*

$$M_{b|(i)} = \frac{\sum_j \hat{\lambda}_{ij}(\hat{P}_{ij}\hat{B}_{ij})^{\delta}}{\sum_j \hat{\lambda}_{ij}(\hat{P}_{ij}\hat{B}_{ij})^{\delta}\ {}_2F_1(b,-\delta;1-\delta;-\theta\hat{B}_{ij}^{-1})}, \quad (8)$$

where $\hat{\lambda}_{ij} = \lambda_j/\lambda_i$, $\hat{P}_{ij} = P_j/P_i$ and $\hat{B}_{ij} = B_j/B_i$.

Proof: This follows directly from the proof of Thm. 1. ■

Corollary 3 (Mean local delay) *For the typical user in the i-th tier, the mean local delay is given by*

$$M_{-1|(i)} = \frac{(1-\delta)\sum_j \hat{\lambda}_{ij}(\hat{P}_{ij}\hat{B}_{ij})^{\delta}}{\sum_j \hat{\lambda}_{ij}(\hat{P}_{ij}\hat{B}_{ij})^{\delta}(1-\delta-\delta\theta\hat{B}_{ij}^{-1})}. \quad (9)$$

Proof: The mean local delay is the -1-st moment of the conditional success probability in Cor. 2. Using the identity ${}_2F_1(-1,b;c;z) \equiv 1 - \frac{bz}{c}$, (9) is obtained. ■

The mean local delay $M_{-1|(i)}$ has a phase transition at $\theta_{\mathrm{c}|(i)}$ as given in (10) when it is seen as a function of the SIR threshold with the other parameters fixed, which means the mean local delay is finite for $\theta < \theta_{\mathrm{c}|(i)}$ and is infinite for $\theta \geq \theta_{\mathrm{c}|(i)}$. By setting the denominator in (9) to zero, we obtain

$$\theta_{\mathrm{c}|(i)} = \frac{(1-\delta)\sum_j \hat{\lambda}_{ij}(\hat{P}_{ij}\hat{B}_{ij})^{\delta}}{\delta\sum_j \hat{\lambda}_{ij}(\hat{P}_{ij})^{\delta}(\hat{B}_{ij})^{\delta-1}}. \quad (10)$$

B. Calculation and Approximation of the Meta Distribution

According to the Gil-Pelaez theorem [21], for a general variable $X > 0$ with characteristic function $\varphi_X(t) \triangleq \mathbb{E}e^{jtX}$, $j \triangleq \sqrt{-1}$, $t \in \mathbb{R}$, the CCDF of X is given by

$$\bar{F}_X(x) = \frac{1}{2} + \frac{1}{\pi}\int_0^{\infty} \frac{\Im(e^{-jt\log x}\varphi_X(jt))}{t}\mathrm{d}t, \quad (11)$$

where $\Im(z)$ denotes the imaginary parts of $z \in \mathbb{C}$.

Letting $X \triangleq \log P_{\mathrm{s}}(\theta)$ (or $X \triangleq \log P_{s|(i)}(\theta)$), we have $\varphi_X(t) = M_{jt}$ (or $\varphi_X(t) = M_{jt|(i)}$), setting $b = jt$ in (7) (or (8)). Hence, the meta distribution of the conditional success probability for the whole network (and the specific i-th tier) can be calculated.

The calculation of the exact meta distribution via the Gil-Pelaez theorem usually involves many calculations of imaginary moments, which prohibits direct insights into the meta distributions and its applications in mapping to other performance metrics like the ergodic data rate [18], etc. An efficient approximation of the meta distribution $\bar{F}(\theta, t)$ is obtained by using the beta distribution through matching the first moment M_1 and second moment M_2, which has been verified in [11], [15]–[18] for various network scenarios. Specifically,

$$\bar{F}(\theta,t) \approx 1 - I_x\Big(\frac{\beta M_1}{1-M_1}, \beta\Big), \ x \in [0,1], \quad (12)$$

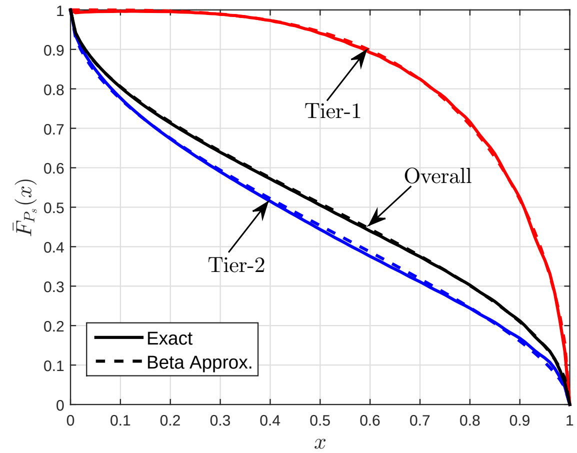

(a) A two-tier HCN

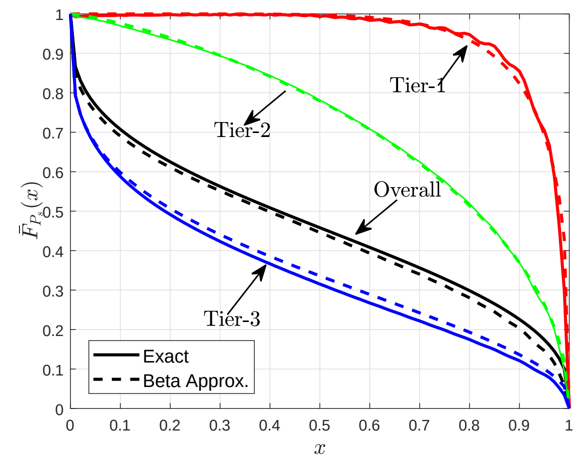

(b) A three-tier HCN

Fig. 1. The exact meta distributions and beta approximations for the overall network and for each tier of (a) a two-tier HCN and (b) a three-tier HCN with $\theta = 0$ dB, $\alpha = 4$, $\lambda_1 = 1$, $\lambda_2 = 5$, $\lambda_3 = 10$, $P_1 = 1$, $P_2 = 0.2$, $P_3 = 0.05$, $B_1 = 0$ dB, $B_2 = 10$ dB and $B_3 = 20$ dB. The solid lines correspond to the exact results and the dashed lines are the beta approximations.

where $\beta = \frac{(M_1-M_2)(1-M_1)}{M_2-M_1^2}$, $I_x(.,.)$ is the regularized incomplete beta function.

It is worth noting that recently, as shown in [22], the (approximate) meta distribution can also be directly obtained from the moments by a simple linear transform, which is a more convenient way for efficient calculations.

Fig. 1(a) shows the meta distributions for a two-tier HCN, and Fig. 1(b) shows the meta distributions for a three-tier network, where the first two tiers are identical to the previous network. First we can see that the beta approximations are excellent for multi-tier HCNs with biases. Moreover, by comparing the two figures, we can observe the influence by increasing the number of tiers from two to three, i.e., the coverage performance of the existing tiers benefit from the offloading provided by the newly deployed tier, while the performance of the latter is below the average of the whole network.

C. Asymptotic SIR Gains

As shown in [12], [23], [24], the CCDFs $\bar{F}_{\mathsf{SIR}}(\theta)$ of the SIR at the typical user in all general single-tier nearest-associated networks resemble merely horizontally shifted versions in the SIR threshold θ (in dB) of each other, as long as they have the same diversity gain. The horizontal gap (or the "SIR gain") relative to a reference network model at the target success probability $p_{\rm t}$ is given by

$$G_{\rm p}(p_{\rm t}) \triangleq \frac{\bar{F}_{\mathsf{SIR}}^{-1}(p_{\rm t})}{\bar{F}_{\mathsf{SIR}_{\rm ref}}^{-1}(p_{\rm t})}, \tag{13}$$

where $\bar{F}_{\mathsf{SIR}}^{-1}$ is the inverse function of $\bar{F}_{\mathsf{SIR}}(\theta)$.

Usually it is more convenient to write $G_{\rm p}(p_{\rm t})$ as a function of θ by $G(\theta) = \theta'/\theta$, where θ' is given by $\bar{F}_{\mathsf{SIR}}(\theta') = \bar{F}_{\mathsf{SIR}_{\rm ref}}(\theta) = p_{\rm t}$.

The asymptotic SIR gain at the high-reliability regime is defined by

$$G_0 \triangleq \lim_{\theta\to 0} G(\theta). \tag{14}$$

Similarly, the asymptotic SIR gain at the low-reliability regime is defined as

$$G_\infty \triangleq \lim_{\theta\to \infty} G(\theta). \tag{15}$$

Usually, the most sensible reference network model is the homogeneous PPP. If G_0 (or G_∞) exists, then a rather convenient way to estimate $p_{\rm s}(\theta)$ of the network in focus is by using G_0 (or G_∞) as the scaling factor G for θ, *i.e.*,

$$p_{\rm s}(\theta) \approx p_{\rm s,PPP}(\theta/G). \tag{16}$$

$G(\theta)$ in dB quantifies the horizontal gap between $p_{\rm s}(\theta)$ and $p_{\rm s,PPP}(\theta)$ for θ in dB.

Next, we extend the above-mentioned SIR asymptotic gain in single-tier networks to HCNs based on the HIP model.

Definition 1 (Asymptotic SIR gains in HCNs) *For the HC-N model in this paper, the asymptotic SIR gains of the b-th moment of the conditional success probability for each tier, at both the high-reliability and low-reliability regimes, with the standard success probability of the single-tier PPP as the reference, are, respectively, given by*

$$G_{0,b}^{(i)} = \lim_{\theta\to 0} \frac{M_{b|(i)}^{-1}(p_{\rm s,PPP}(\theta))}{\theta}, \tag{17}$$

and

$$G_{\infty,b}^{(i)} = \lim_{\theta\to \infty} \frac{M_{b|(i)}^{-1}(p_{\rm s,PPP}(\theta))}{\theta}. \tag{18}$$

where $M_{b|(i)}^{-1}$ is the inverse function of $M_{b|(i)}$ and $p_{\rm s,PPP}(\theta) = M_1$ in (7).

We will show that, remarkably, the horizontal shift is applicable to each tier in the HCN. Before deriving the asymptotic gains, we first state a lemma about the asymptotics of the hypergeometric function ${}_2F_1$.

Lemma 2 *For $b \in \mathbb{C}$,*

$$ {}_2F_1(b,-\delta;1-\delta;-z) \sim 1 + bz\frac{\delta}{1-\delta}, \quad z\to 0, \tag{19}$$

and

$$ {}_2F_1(b,-\delta;1-\delta;-z) \sim z^\delta T(b), \quad z\to \infty, \tag{20}$$

where $T(b) = \int_0^\infty (1-(1+r^{-\frac{1}{\delta}})^{-b})\mathrm{d}r$.

Proof: For $z\to 0$, (19) simply follows from the definition (*i.e.*, the series expression) of the hypergeometric function ${}_2F_1(a,b;c;z) \triangleq \sum_{n=0}^{\infty} \frac{(a)_n (b)_n}{(c)_n}\frac{z^n}{n!}$, for $|z|<1$ and $(q)_m \triangleq \frac{\Gamma(q+m)}{\Gamma(q)}$ is the Pochhammer function (rising factorial).

When $z\to\infty$, we express the hypergeometric function as

$$\begin{aligned} {}_2F_1(-b,-\delta;1-\delta;-z) &= 1 + 2\int_0^1 \Big(1-\frac{1}{(1+zr^\alpha)^b}\Big) r^{-3}\mathrm{d}r \\ &= 1 + z^\delta 2\int_0^{z^{\frac{1}{\alpha}}} \Big(1-\frac{1}{(1+r^\alpha)^b}\Big) r^{-3}\mathrm{d}r \\ &= 1 + z^\delta \int_{z^{-\frac{1}{\delta}}}^{\infty} \Big(1-\frac{1}{(1+r^{-\frac{1}{\delta}})^b}\Big)\mathrm{d}r \\ &= 1 + z^\delta\Big(T(b) - f(z)\Big), \end{aligned} \tag{21}$$

where $f(z) = \int_0^{z^{-1/\delta}} \big(1-\frac{1}{(1+r^{-1/\delta})^b}\big)\mathrm{d}r$. The first step is according to [11, eq. (23)]; the second step follows from the variable substitution $z^{\frac{1}{\alpha}} r \to r$ and $\delta = 2/\alpha$; the third step follows from the variable substitution $r \to r^{-\frac{1}{2}}$.

Since $f(z) = o(1)$ as $z\to\infty$, only the term $T(b)$ matters asymptotically after multiplication with z^δ, *i.e.*, $z^\delta(T(b) - o(1)) \sim z^\delta T(b)$, and we obtain (20). ∎

Corollary 4 (Asymptotic SIR gains relative to PPP) *Conditioned on the typical user connecting to the i-th tier, the asymptotic SIR gains of the b-th moment of the meta distribution relative to M_1 of the single-tier homogeneous PPP are given by*

$$G_{0,b}^{(i)} = \frac{\sum_j \hat{\lambda}_{ij}\hat{P}_{ij}^\delta \hat{B}_{ij}^\delta}{b\sum_j \hat{\lambda}_{ij}\hat{P}_{ij}^\delta \hat{B}_{ij}^{\delta-1}}, \tag{22}$$

and

$$G_{\infty,b}^{(i)} = \Big(\frac{T(1)}{T(b)}\frac{\sum_j \hat{\lambda}_{ij}\hat{P}_{ij}^\delta \hat{B}_{ij}^\delta}{\sum_j \hat{\lambda}_{ij}\hat{P}_{ij}^\delta}\Big)^{\frac{1}{\delta}}, \tag{23}$$

where $b\in\mathbb{C}$, $\hat{\lambda}_{ij} = \lambda_j/\lambda_i$, $\hat{P}_{ij} = P_j/P_i$ and $\hat{B}_{ij} = B_j/B_i$.

Proof: To determine $G_{0,b}^{(i)}$, we need to evaluate the limit of $M_{b|(i)}(\theta)$ at $\theta\to 0$. Applying (19) in (8),

$$\begin{aligned} M_{b|(i)}(\theta) &\sim \frac{\sum_j \hat{\lambda}_{ij}\hat{P}_{ij}^\delta \hat{B}_{ij}^\delta}{\sum_j \hat{\lambda}_{ij}\hat{P}_{ij}^\delta \hat{B}_{ij}^\delta\Big(1 + b\theta\hat{B}_{ij}^{-1}\frac{\delta}{1-\delta}\Big)} \\ &= \frac{1}{1+\frac{\delta}{1-\delta}\frac{\theta}{G_{0,b}^{(i)}}} \\ &\sim 1 - \frac{\delta}{1-\delta}\frac{\theta}{G_{0,b}^{(i)}}. \end{aligned} \tag{24}$$

Since for the PPP,

$$M_{1,\rm PPP}(\theta) = \frac{1}{{}_2F_1(1,-\delta,1-\delta;-\theta)} \sim 1 - \frac{\theta\delta}{1-\delta}, \tag{25}$$

it is clear that $G_{0,b}^{(i)}$ is exactly the asymptotic gain for $\theta \to 0$.

To determine $G_{\infty,b}^{(i)}$, applying (20) in (7) and (8), we have

$$M_{1,\mathrm{PPP}}(\theta) \sim \theta^{-\delta} T^{-1}(1), \tag{26}$$

$$M_{b|(i)}(\theta) \sim \Big(\frac{\sum_j \hat{\lambda}_{ij} \hat{P}_{ij}^{\delta}}{\sum_j \hat{\lambda}_{ij} \hat{P}_{ij}^{\delta} \hat{B}_{ij}^{\delta}} T(b) \theta^{\delta} \Big)^{-1}. \tag{27}$$

$G_{\infty,b}^{(i)}$ is then obtained by comparing (26) and (27). ■

Remark 2 *In Cor. 4, the reference model in use is the first moment of the conditional success probability of the single-tier PPP. Another possibility is to use the b-th moment of the conditional success probability of the single-tier PPP as the reference model; in this case, the two asymptotic gains in* (22) *and* (23) *become* ${G'}_{0,b}^{(i)}$ *and* ${G'}_{\infty,b}^{(i)}$*, which are constants as shown in* (28) *and* (29)*, respectively.*

$${G'}_{0,b}^{(i)} = \frac{\sum_j \hat{\lambda}_{ij} \hat{P}_{ij}^{\delta} \hat{B}_{ij}^{\delta}}{\sum_j \hat{\lambda}_{ij} \hat{P}_{ij}^{\delta} \hat{B}_{ij}^{\delta-1}}, \tag{28}$$

$${G'}_{\infty,b}^{(i)} = \Big(\frac{\sum_j \hat{\lambda}_{ij} \hat{P}_{ij}^{\delta} \hat{B}_{ij}^{\delta}}{\sum_j \hat{\lambda}_{ij} \hat{P}_{ij}^{\delta}} \Big)^{\frac{1}{\delta}}. \tag{29}$$

From this it is easy to infer that the variances $V^{(i)}(\theta)$ *of each tier are also shifted versions of each other, as shown in Fig. 5 in Sec. IV.*

D. Base Station Activity

In this section, we model the random activities of interfering base stations in each tier by the ALOHA model, *i.e.*, the interfering BSs of tier i are active only with probability p_i. The activities of different base stations are independent. We first derive the general b-th moment for the typical user of each individual tier and the whole network and then a lower bound of the activity probabilities that result in finite mean local delay.

Theorem 2 *Given that the typical user connects to the* i*-th tier with the serving BS always being active, and the interfering BSs in tier* $j \in [K]$ *are active independently with probability* p_j*, the b-th moment of the meta distribution can be expressed as* (30)*, where* $\boldsymbol{p} = (p_1, p_2, ...p_K)$*,* $\hat{\lambda}_{ij} = \lambda_j/\lambda_i$*,* $\hat{P}_{ij} = P_j/P_i$*, and* $\hat{B}_{ij} = B_j/B_i$*.*

Proof: See Appendix B. ■

As expected, letting $K = 1$, (30) retrieves the single-tier result in [11, Thm. 3]; also, letting $K = 2$ and assuming the two tiers share the same parameters, the result of each tier is also the same as the-single tier result.

Theorem 3 *For the overall typical (active) user with the interfering BSs in tier* $j \in [K]$ *are active independently with probability* p_j*, the b-th moment of the meta distribution can be expressed as* (31)*, where* $\boldsymbol{p} = (p_1, p_2, ...p_K)$*,* $\hat{\lambda}_{ij} = \lambda_j/\lambda_i$*,* $\hat{P}_{ij} = P_j/P_i$*, and* $\hat{B}_{ij} = B_j/B_i$*.*

From (30), the mean local delay of the typical user connecting to the i-th tier is given by

$$M_{-1|(i)}(\boldsymbol{p}) = \frac{1}{D_i(\boldsymbol{p})}, \quad \boldsymbol{p} \in \mathcal{S}_i, \tag{32}$$

where

$$\begin{aligned} D_i(\boldsymbol{p}) = 1 &- \frac{p_i \theta \delta}{1-\delta} \, {}_2F_1(1, 1-\delta; 2-\delta; -\theta(1-p_i)) \\ &+ \sum_{j \neq i} \frac{\lambda_j}{\lambda_i} \Big(\frac{P_j B_j}{P_i B_i} \Big)^{\delta} \Big(1 - \frac{p_j \theta \delta}{1-\delta} \\ &\cdot {}_2F_1\Big(1, 1-\delta; 2-\delta; -\frac{\theta B_i (1-p_j)}{B_j}\Big) \Big), \end{aligned} \tag{33}$$

and $\mathcal{S}_i$ is the region for $\boldsymbol{p}$ in which the mean local delay is finite for the i-th tier, defined by

$$\mathcal{S}_i \triangleq \{(p_1, p_2, ...p_K) \in [0,1]^K : D_i(\boldsymbol{p}) > 0\}. \tag{34}$$

The boundary of the region for the finite mean local delay for the i-th tier is then defined as

$$\partial \mathcal{S}_i \triangleq \{(p_1, p_2, ...p_K) \in [0,1]^K : D_i(\boldsymbol{p}) = 0\}. \tag{35}$$

The region of all tiers is then given by the intersection

$$\mathcal{S} \triangleq \bigcap_{i \in [K]} \mathcal{S}_i. \tag{36}$$

A simple but reasonable inference from (32) and (33) is that for small $\boldsymbol{p}$, the mean local delay is finite since the interference is low and most of the users in each tier have a high conditional success probability, as $\boldsymbol{p}$ grows higher, the interference gets severe, and with $\boldsymbol{p}$ increasing to some critical threshold, $D_i(\boldsymbol{p})$ will go to zero, resulting in the infinite mean local delay.

It is hard to exactly characterize $\mathcal{S}_i$, next we provide a lower bound $\partial \check{\mathcal{S}}_i$ of $\mathcal{S}_i$ to shed light on the effect of the base station activity probabilities $\boldsymbol{p}$. By noticing that

$$\begin{aligned} {}_2F_1(1, 1-\delta; 2-\delta; -z) &\overset{\text{(a)}}{=} (1+z)^{-1} \, {}_2F_1\Big(1, 1; 2-\delta; \frac{z}{1+z}\Big) \\ &\overset{\text{(b)}}{=} (1+z)^{-1} \sum_{m=0}^{\infty} \frac{(1)_m (1)_m}{(2-\delta)_m} \frac{u^m}{m!} \\ &= (1+z)^{-1} \sum_{m=0}^{\infty} \frac{(1)_m}{(2-\delta)_m} u^m \\ &< (1+z)^{-1} \Big(1 + \frac{u}{2-\delta} + \frac{u^2}{2-\delta} + ... \Big) \\ &= (1+z)^{-1} \Big(1 + \frac{1}{2-\delta} \frac{u}{1-u} \Big) \\ &= (1+z)^{-1} \Big(1 + \frac{1}{2-\delta} z \Big), \end{aligned} \tag{37}$$

where (a) is by the Euler's transformation; (b) is by the series form of the Gaussian hypergeometric function ${}_2F_1$ and $(q)_m \equiv \frac{\Gamma(q+m)}{\Gamma(q)}$ is the Pochhammer function (rising factorial). The boundary is given by

$$\partial \check{\mathcal{S}}_i = \{(p_1, p_2, ...p_K) \in [0,1]^K : \check{D}_i(\boldsymbol{p}) = 0\}, \tag{38}$$

$$M_{b|(i)}(\boldsymbol{p}) = \frac{\sum_j \hat{\lambda}_{ij}(\hat{P}_{ij}\hat{B}_{ij})^\delta}{\sum\limits_j \hat{\lambda}_{ij}(\hat{P}_{ij}\hat{B}_{ij})^\delta\big(1 - \sum\limits_{k=1}^{\infty} \binom{b}{k}(-p_j\theta\hat{B}_{ij}^{-1})^k \frac{\delta}{k-\delta}\ {}_2F_1(k, k-\delta; k-\delta+1; -\theta\hat{B}_{ij}^{-1})\big)} \tag{30}$$

$$M_b(\boldsymbol{p}) = \sum_i \frac{1}{\sum\limits_j \hat{\lambda}_{ij}(\hat{P}_{ij}\hat{B}_{ij})^\delta\big(1 - \sum\limits_{k=1}^{\infty} \binom{b}{k}(-p_j\theta\hat{B}_{ij}^{-1})^k \frac{\delta}{k-\delta}\ {}_2F_1(k, k-\delta; k-\delta+1; -\theta\hat{B}_{ij}^{-1})\big)} \tag{31}$$

where

$$\check{D}_i(\boldsymbol{p}) = \sum_j \frac{\lambda_j}{\lambda_i}\Big(\frac{P_jB_j}{P_iB_i}\Big)^\delta\Big(1-\frac{p_j\theta\delta}{1-\delta}\Big(1+\theta\frac{B_i}{B_j}(1-p_j)\Big)^{-1}\Big(1+\frac{\theta B}{(2}$$

(39)

IV. Applications in Two-tier HCNs

In this section, we apply the meta distribution framework developed in Sec. III to the two-tier HIP model and show the corresponding numerical results. Since the performances are affected only by the ratios between the densities, transmit powers and biases of the two tiers, we assume $P_1 = \lambda_1 = B_1 = 1$ without loss of generality.

A. Moments

Defining $f_b(x) \triangleq {}_2F_1(b, -\delta; 1-\delta; -x)$, we obtain the first moment and variance for each tier from Cor. 2,

$$M_{1|(1)} = \frac{1 + \lambda_2(P_2B_2)^\delta}{f_1(\theta) + \lambda_2(P_2B_2)^\delta\ f_1(\theta B_2^{-1})}, \tag{40}$$

$$M_{1|(2)} = \frac{1 + \lambda_2^{-1}(P_2B_2)^{-\delta}}{f_1(\theta) + \lambda_2^{-1}(P_2B_2)^{-\delta}\ f_1(\theta B_2)}, \tag{41}$$

$$V_{(1)} = \frac{1 + \lambda_2(P_2B_2)^\delta}{f_2(\theta) + \lambda_2(P_2B_2)^\delta\ f_2(\theta B_2^{-1})} - \Big(\frac{1 + \lambda_2(P_2B_2)^\delta}{f_1(\theta) + \lambda_2(P_2B_2)^\delta\ f_1(\theta B_2^{-1})}\Big)^2, \tag{42}$$

$$V_{(2)} = \frac{1 + \lambda_2^{-1}(P_2B_2)^{-\delta}}{f_2(\theta) + \lambda_2^{-1}(P_2B_2)^{-\delta}\ f_2(\theta B_2)} - \Big(\frac{1 + \lambda_2^{-1}(P_2B_2)^{-\delta}}{f_1(\theta) + \lambda_2^{-1}(P_2B_2)^{-\delta}\ f_1(\theta B_2)}\Big)^2. \tag{43}$$

Fig. 2 and Fig. 3 show M_1 and V of each tier in a two-tier HCN. We can see that if there is no bias (*i.e.*, $B_1 = B_2 = 1$), the curves of M_1 and V of both tiers coincide, which implies that the two tiers have the same SIR statistics regardless of their different densities and powers. However, the inequality in range expansion bias results in the separation between these two tiers in terms of M_1 and V. Specifically, since biasing means offloading, we can draw the conclusion that offloading from one tier to the other will always benefit M_1 of the former, while harming the latter, for any given θ.

B. Horizontal Shifting via Asymptotic SIR Gains

For the two-tier HCN example (the same one for Fig. 1(a)), the asymptotic SIR gain for M_1 of each tier is respectively

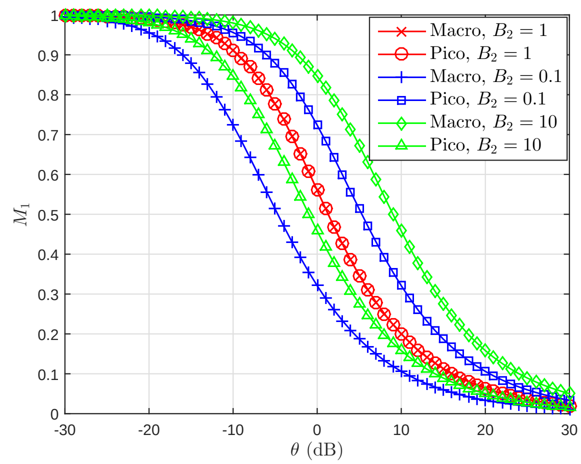

Fig. 2. M_1 of the typical user in each tier versus θ with $\alpha = 4$, $P_2 = 0.2$ and $\lambda_2 = 5$. In this case, for $B_2 = 1$, $p_a^{(1)} = 0.5$ and $p_a^{(2)} = 0.5$; for $B_2 = 0.1$, $p_a^{(1)} = 0.59$ and $p_a^{(2)} = 0.41$; for $B_2 = 10$, $p_a^{(1)} = 0.12$ and $p_a^{(2)} = 0.88$.

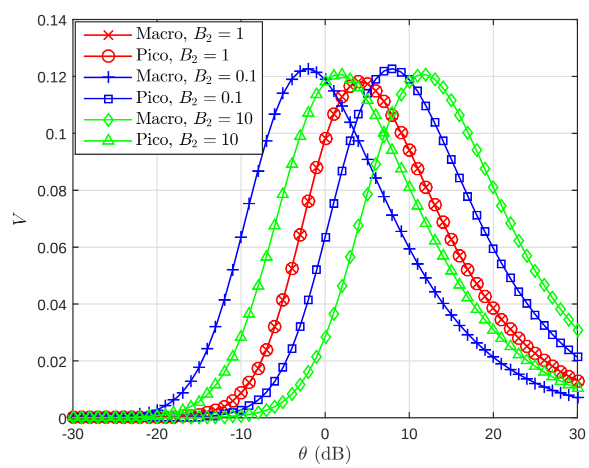

Fig. 3. V of the typical user in each tier versus θ with $\alpha = 4$, $P_2 = 0.2$ and $\lambda_2 = 5$. In this case, for $B_2 = 1$, $p_a^{(1)} = 0.5$ and $p_a^{(2)} = 0.5$; for $B_2 = 0.1$, $p_a^{(1)} = 0.59$ and $p_a^{(2)} = 0.41$; for $B_2 = 10$, $p_a^{(1)} = 0.12$ and $p_a^{(2)} = 0.88$.

given by $G_{0,1}^{(1)} = \frac{1+\lambda_2P_2^\delta B_2^\delta}{1+\lambda_2P_2^\delta B_2^{\delta-1}}$ and $G_{0,1}^{(2)} = \frac{1+\lambda_2^{-1}P_2^{-\delta}B_2^{-\delta}}{1+\lambda_2^{-1}P_2^{-\delta}B_2^{1-\delta}}$. Numerically, for the case $B_2 = 10$ dB shown in Fig. 2 and Fig. 3, $G_{0,1}^{(1)} = 6.75$ dB, $G_{0,1}^{(2)} = -3.25$ dB, $G_{0,2}^{(1)} = 3.74$ dB, $G_{0,2}^{(2)} = -6.27$ dB, $G_{\infty,1}^{(1)} = 9.94$ dB, $G_{\infty,1}^{(2)} = -2.06$ dB, $G_{\infty,2}^{(1)} = 4.42$ dB and $G_{\infty,2}^{(2)} = -5.58$ dB. Fig. 4 shows

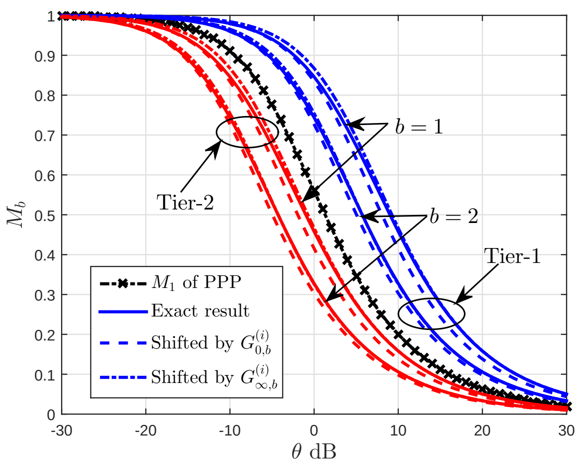

Fig. 4. Illustration for the asymptotic gain of M_b in each tier of a two-tier HCN relative to M_1 of a single-tier PPP. In this case, $\alpha=4$, $P_2=0.2$ and $\lambda_2=5$, $B_2=10$ dB. The solid lines correspond to the exact results and the dashed lines are the shifted versions of M_1 of the single-tier PPP by $G^{(i)}_{0,b}$ and $G^{(i)}_{\infty,b}$, $i=1,2$, respectively.

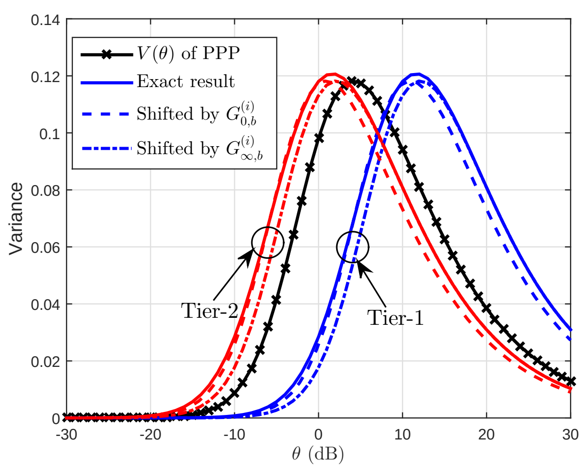

Fig. 5. Illustration for the asymptotic gain of $V^{(i)}(\theta)$ of a two-tier HCN relative to the variance of a single-tier PPP. In this case, $\alpha=4$, $P_2=0.2$ and $\lambda_2=5$, $B_2=10$ dB. The solid lines correspond to the exact results and the dashed lines are the shifted versions of $V(\theta)$ of the single-tier PPP by the asymptotic gains $G^{(i)}_{0,b}$ and $G^{(i)}_{\infty,b}$, $i=1,2$, respectively.

the comparison between the exact b-th moment curves and the shifted versions of the M_1 of a single-tier PPP as the reference model and Fig. 5 shows the comparison between the exact variance curves and the shifted versions of the variance of a single-tier PPP as the reference model. We can see that the shifted versions by using the asymptotic gain are excellent approximations for the exact results.

C. Effects of Biasing

In this section, we study the effects of range expansion biases on the coverage performance of each individual tier and the whole network.

Sometimes, it is convenient and of significance to consider the asymptotic performance of the range expansion biases.

Corollary 5 *For $B_2\to\infty$, which means that tier 1 is closed-access, we have*

(a) $M_{1|(1)}\sim 1,\ M_{1|(2)}\sim \dfrac{\lambda_2 P_2^\delta \operatorname{sinc}\delta}{F(\delta,\theta)\lambda_2 P_2^\delta\operatorname{sinc}\delta+\theta^\delta}$*; further, for* $\theta\to\infty,\ M_{1|(2)}\sim\dfrac{\lambda_2 P_2^\delta\operatorname{sinc}\delta}{\theta^\delta(1+\lambda_2P_2^\delta)}$;

(b) $V_{(1)}\to 0,\ V_{(2)}\sim \dfrac{1}{F(\delta,\theta)+\frac{3-2\delta}{(2-\delta)\lambda_2P_2^\delta\operatorname{sinc}\delta}\theta^\delta}-\left(\dfrac{\lambda_2P_2^\delta\operatorname{sinc}\delta}{F(\delta,\theta)\lambda_2P_2^\delta\operatorname{sinc}\delta+\theta^\delta}\right)^2$*; further, for* $\theta\to\infty,\ V_{(2)}\sim \dfrac{\lambda_2P_2^\delta\operatorname{sinc}\delta}{\theta^\delta(1+\delta)(1+\lambda_2P_2^\delta)}-\dfrac{\lambda_2^2P_2^{2\delta}\operatorname{sinc}^2\delta}{\theta^{2\delta}(1+\lambda_2P_2^\delta)^2}$,

where $F(\delta,\theta)={}_2F_1(1,-\delta;1-\delta;-\theta)$.

Proof: These results are easily obtained by using (20) in Lemma 2 by noting that $T(1)=\frac{1}{\operatorname{sinc}\delta}$, $T(2)=\frac{1+\delta}{\operatorname{sinc}\delta}$ and the identity ${}_2F_1(a,b;c;0)\equiv 1$. ■

Corollary 6 $B_2>1\Leftrightarrow M_{1|(1)}>M_{1|(2)}$.

Proof: Since $f_1(x)$ is monotonically increasing, we have $f_1(\theta B_2)>f_1(\theta)>f_1(\theta B_2^{-1})$ for $B_2>1$. Then from (40) and (41) we have $M_{1|(1)}>\frac{1}{1+f_1(\theta)}$ while $M_{1|(2)}<\frac{1}{1+f_1(\theta)}$. ■

In words, offloading from one tier to the other will harm the average success probability of the latter tier.

As for the overall typical user, according to Thm. 1, its first moment and variance of the conditional success probability are, respectively, given by

$$M_1(B_2)=\frac{1}{f_1(\theta)+\lambda_2(P_2B_2)^\delta f_1(\theta B_2^{-1})}+\frac{1}{f_1(\theta)+\lambda_2^{-1}(P_2B_2)^{-\delta}f_1(\theta B_2)},\tag{44}$$

$$V(B_2)=\frac{1}{f_2(\theta)+\lambda_2(P_2B_2)^\delta f_2(\theta B_2^{-1})}+\frac{1}{f_2(\theta)+\lambda_2^{-1}(P_2B_2)^{-\delta}f_2(\theta B_2)}-\left(\frac{1}{f_1(\theta)+\lambda_2(P_2B_2)^\delta f_1(\theta B_2^{-1})}+\frac{1}{f_1(\theta)+\lambda_2^{-1}(P_2B_2)^{-\delta}f_1(\theta B_2)}\right)^2.\tag{45}$$

We can prove that $\left.\frac{\partial M_1}{\partial B_2}\right|_{B_2=1}=0$, $\left.\frac{\partial V}{\partial B_2}\right|_{B_2=1}=0$, which means $B_2=1$ is an extreme point. Also, $\left.\frac{\partial^2 M_1}{\partial B_2^2}\right|_{B_2=1}\le 0$, hence $B_2=1$ is the maximal point of M_1 (see that shown in Fig. 6). For the second derivative of V at $B_2=1$, it is not easy to judge its sign across different values of B_2 since it is related to the value of θ. But we can observe this from the analytical curves shown in Fig. 7 that $B_2=1$ is the local minimum.

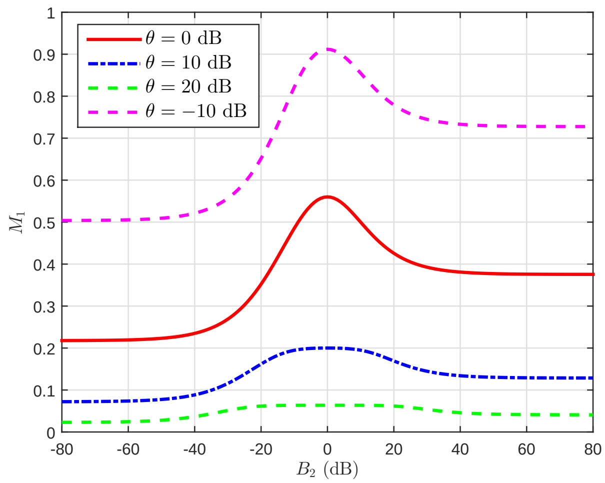

Fig. 6. Analytical results for M_1 of the typical user of the entire network versus B_2 with $\alpha = 4$, $P_2 = 0.2$ and $\lambda_2 = 4$.

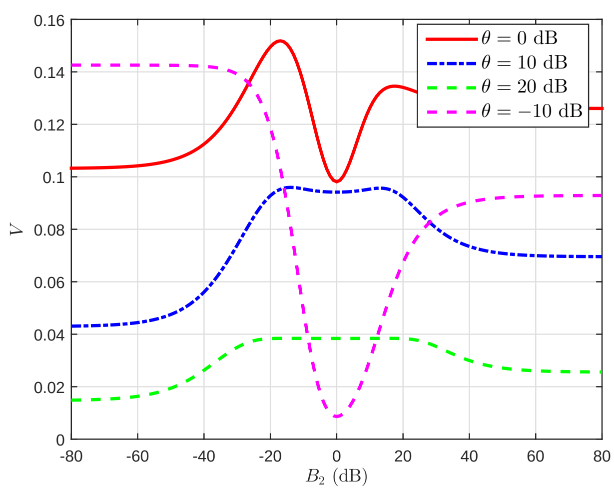

Fig. 7. Analytical results for V of the typical user of the entire network versus B_2 with $\alpha = 4$, $P_2 = 0.2$ and $\lambda_2 = 4$.

Based on the above analysis, for the M_1 of the overall users in a general K-tier HCN, we have the following corollary.

Corollary 7 *For the K-tier HIP model, setting all bias terms B_i to the same value (i.e., no biasing) maximizes $M_1(\theta)$ of the overall typical user for all $\theta > 0$.*

Proof: For an arbitrary realization of the point process Ψ, determine the local-average SIR, which is equal to (2) but without the fading coefficients (see [25, Eqn. (11)]) for all users for $B_i = 1, i \in [K]$ (no biasing). This is by definition the best local-average SIR that each user can achieve. Consequently, if for any tier i, $B_i \neq 1$, there will be some users whose local-average SIR will decrease since they are no longer associated with the strongest-on-average BS. This implies that M_1 decreases. ■

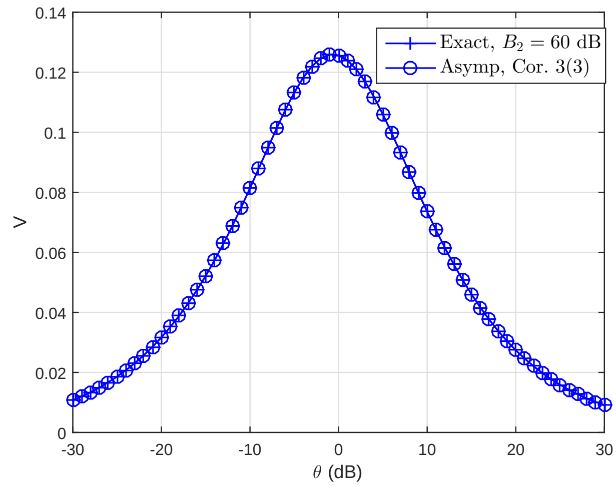

Fig. 8. Asymptotic V of the typical user in the pico tier versus θ with $\alpha = 4$, $P_2 = 0.2$ and $\lambda_2 = 5$.

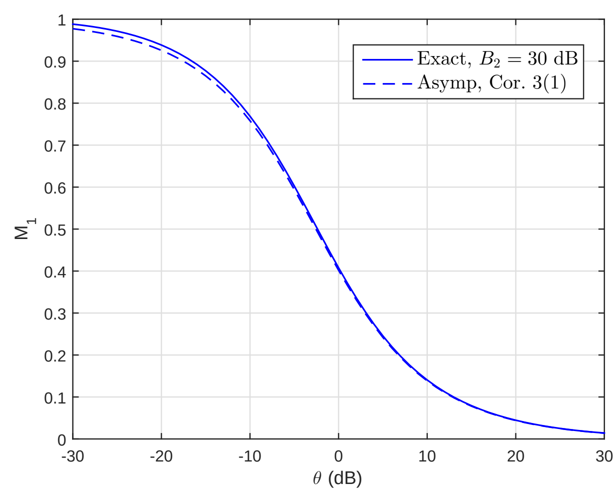

Fig. 9. Asymptotic M_1 of the typical user in the pico tier versus θ with $\alpha = 4$, $P_2 = 0.2$ and $\lambda_2 = 5$.

Remark 3 *For a general K-tier HCN with range expansion bias B_i in the i-th tier, it is not easy to determine whether $B_i > 1$ is harmful to the coverage performance in terms of M_1 for the i-th tier than the case with $B_i = 1$. Since what plays the decisive role are the ratios between B_i and the bias values of the other tiers, which, in essence, reflect the offloading relationship among different tiers. In particular, $B_i/B_j < 1$ means offloading from the i-th tier to the j-th tier and vice versa. Hence, for a two-tier case, if some of the users in the first tier are offloaded to the second tier, then the latter definitely suffers a loss in M_1; however, for a three-tier case, if some of the users in the first tier are offloaded to the second tier, but some users belong to the second tier are also offloaded to the third tier, then the M_1 of the second tier may improve.*

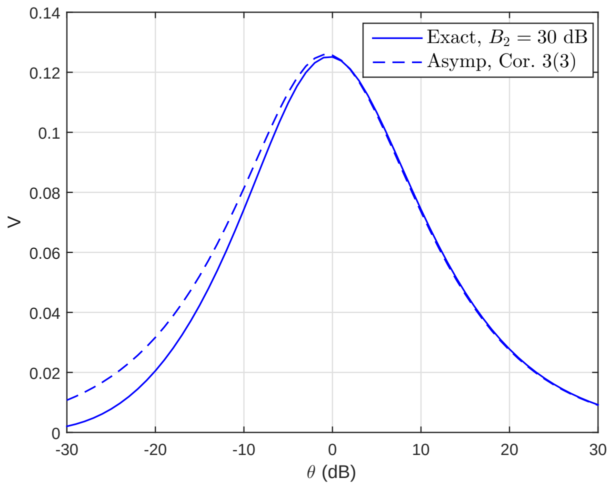

Fig. 10. Asymptotic V of the typical user in the pico tier versus θ with $\alpha = 4$, $P_2 = 0.2$ and $\lambda_2 = 5$.

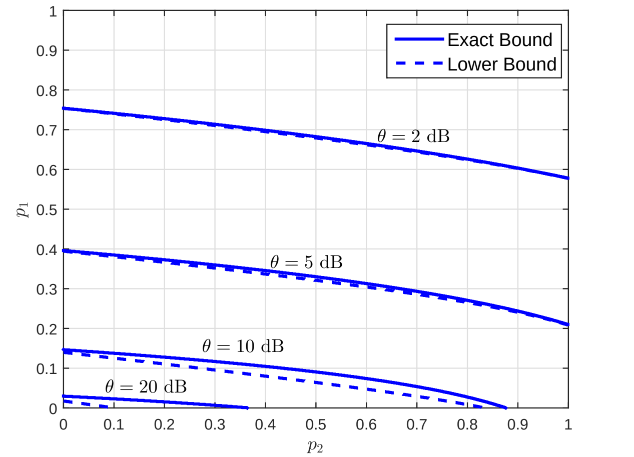

Fig. 11. The exact boundary $\partial\mathcal{S}_1$ and its lower bound $\partial\check{\mathcal{S}}_1$ of a two-tier HCN with $\alpha = 4$, $\lambda_2/\lambda_1 = 25$, $P_1/P_2 = 200$ and $B_2/B_1 = 10$. In this case, $\mathcal{S} = \mathcal{S}_1$.

D. Lower Bounds of the Mean Local Delay with Random BS Activity

Specifically, for a two-tier HIP model, we have the following corollary.

Corollary 8 *For a two-tier HCN, given all the other parameters,*

(1) if $B_1 = B_2$, then $\mathcal{S} = \mathcal{S}_1 = \mathcal{S}_2$;
(2) if $B_i > B_j$, then $\mathcal{S} = \mathcal{S}_j$, $i, j \in \{1, 2\}$;
(3) if $\theta < \frac{1-\delta}{\delta}$, then $\mathcal{S} = \mathcal{S}_1 = \mathcal{S}_2 = [0, 1]^2$.

Proof: For a two-tier HCN, we have

$$D_1(p_1, p_2) = \underbrace{1 - \frac{p_1\theta\delta}{1-\delta}\,{}_2F_1(1, 1-\delta; 2-\delta; -\theta(1-p_1))}_{A_1} + \frac{\lambda_2}{\lambda_1}\Big(\frac{P_2B_2}{P_1B_1}\Big)^{\delta} \cdot \Bigg(\underbrace{1 - \frac{p_2\theta\delta}{1-\delta}\,{}_2F_1\Big(1, 1-\delta; 2-\delta; -\theta(1-p_2)\frac{B_1}{B_2}\Big)}_{G_2}\Bigg), \tag{46}$$

$$D_2(p_1, p_2) = \underbrace{1 - \frac{p_2\theta\delta}{1-\delta}\,{}_2F_1(1, 1-\delta; 2-\delta; -\theta(1-p_2))}_{G_1} + \frac{\lambda_1}{\lambda_2}\Big(\frac{P_1B_1}{P_2B_2}\Big)^{\delta} \cdot \Bigg(\underbrace{1 - \frac{p_1\theta\delta}{1-\delta}\,{}_2F_1\Big(1, 1-\delta; 2-\delta; -\theta(1-p_1)\frac{B_2}{B_1}\Big)}_{A_2}\Bigg). \tag{47}$$

(1) For $B_1 = B_2$, let $g(x) = 1 - \frac{x\theta\delta}{1-\delta}\,{}_2F_1(1, 1-\delta; 2-\delta; -\theta(1-x))$, $c = \frac{\lambda_2}{\lambda_1}\big(\frac{P_2}{P_1}\big)^{\delta}$, then $D_1(p_1, p_2) = g(p_1) + cg(p_2)$, $D_2(p_1, p_2) = \frac{D_1(p_1, p_2)}{c}$, since $c > 0$, it is obvious that $D_1(p_1, p_2)$ and $D_2(p_1, p_2)$ always get negative at the same (p_1, p_2). Hence $\mathcal{S}_1$ and $\mathcal{S}_2$ share the same boundary and thus $\mathcal{S}_1 = \mathcal{S}_2$.

(2) Without loss of generality, we assume $B_2 > B_1$. Let $d = \frac{B_2}{B_1} > 1$, then $D_1(p_1, p_2) = A_1 + cd^{\delta}G_2$, $D_2(p_1, p_2) = \frac{A_2 + cd^{\delta}G_1}{cd^{\delta}}$. Since ${}_2F_1(1, 1-\delta; 2-\delta; -z)$ is a monotonically decreasing function of z for $z \geq 0$, which is easy to be proved by its first-order derivative, for given p_1, p_2, we have $A_1 < A_2$, $G_1 > G_2$, hence as p_1 and (or) p_2 increase, $D_1(p_1, p_2)$ will decrease to zero first, resulting in $\mathcal{S}_1 \subset \mathcal{S}_2$.

(3) Let $p_1 = p_2 = 1$, then $\check{D}_i(1, 1) = \big(1 + \sum_{j \neq i} \frac{\lambda_j}{\lambda_i}\big(\frac{P_jB_j}{P_iB_i}\big)^{\delta}\big)\big(1 - \theta\frac{\delta}{1-\delta}\big)$, $\check{D}_i(1, 1) > 0$ requires $\theta < \frac{1-\delta}{\delta}$. ∎

In Fig. 11, the exact boundary $\partial\mathcal{S}_1$ and its lower bound $\partial\check{\mathcal{S}}_1$ of a two-tier HCN are shown. As we see, the lower bound becomes tighter as θ decreases. In this case, according to Cor. 8(2), $\mathcal{S} = \mathcal{S}_1$. We also observe that as θ decreases, $\mathcal{S}$ grows towards $[0, 1]^2$, as expected.

V. Conclusions

In this paper, we developed the SIR meta distribution framework for the analysis of HIP-based K-tier HCNs with offloading biases and Rayleigh fading and performed a systematic study for a series of key performance metrics, revealing fine-grained information on the per-user performance. We first derived the b-th moment of the conditional success probability for both the entire network and each single tier. Based on the b-th moment, the exact meta distribution as well as a simple yet accurate approximation based on beta distribution is provided. We derived the asymptotic gains and found that for any specific tier, the b-th moment as well as the variance of the conditional success probability is approximately a horizontal shifted version of that in a single-tier PPP, and hence horizontal shifted versions of each other.

About the effect of the offloading biases, we proved that M_1 of the whole network is always harmed by any biasing; for multi-tier (more than 3) HIP-based HCNs, users of certain tiers will benefit while the others suffer, depending on the ratios of the biases between different tiers. The effect on the per-tier success probability can be quantified using a horizontal shift of the SIR distribution.

The b-th moment of the conditional success probability under the independent ALOHA-like random base station activities was also addressed. The region of the activity probabilities in which the mean local delay of each tier remains finite is characterized by a lower bound, which was shown to be quite accurate compared to the exact one.

Overall, the SIR meta distribution framework offers several new and interesting insights in the performance of HCNs, which helps us understand the HCNs better and hence benefits the real network design and optimization.

Appendix

A. Proof of Theorem 1

Proof: Let $M_{b|(i)}$ denote the conditional b-th moment of the SIR meta distribution given that the typical user at the origin connects to the i-th tier. Then we have

$$M_b = \sum_{i\in[K]} p_{\mathrm{a}}^{(i)} \cdot M_{b|(i)}. \tag{48}$$

Next, we derive the conditional b-th moment $M_{b|(i)}$.

Given R_i and that the typical user at the origin connects to the i-th tier, the conditional success probability is given by

$$\begin{aligned} &P_{\mathrm{s}}^{(i)}(\theta) \\ &= \mathbb{P}\Bigg(\frac{P_i h_o R_i^{-\alpha}}{\sum\limits_{j\neq i}\sum\limits_{\mathrm{x}\in\Phi_j} P_j h_{\mathrm{x}} R_{\mathrm{x}}^{-\alpha} + \sum\limits_{\mathrm{x}\in\Phi_i\setminus\{\mathrm{x}_0^{(i)}\}} P_i h_{\mathrm{x}} R_{\mathrm{x}}^{-\alpha}} > \theta\Bigg), \end{aligned} \tag{49}$$

where R_i is the distance from the typical user to the nearest BS $\mathrm{x}_0^{(i)}$ in the i-th tier, and h_o is the fading coefficient associated with the link from $\mathrm{x}_0^{(i)}$ to the typical user.

By averaging over the fading, we get the conditional b-th moment of the conditional success probability, given by

$$M_{b|(i),R_i} = \prod_{\mathrm{x}\in\Phi_i}\frac{1}{\left(1+\theta\left(\frac{R_i}{R_{\mathrm{x}}}\right)^{\alpha}\right)^b}\prod_{j\neq i}\prod_{\mathrm{x}\in\Phi_j}\frac{1}{\left(1+\theta\hat{P}_{ij}\left(\frac{R_i}{R_{\mathrm{x}}}\right)^{\alpha}\right)^b}. \tag{50}$$

The notation $M_{b|(i),R_i}$ is used to denote that the b-th moment is conditioned on R_i and the event that the typical user connects to the i-th tier given R_i, which occurs with the probability given in (4).

By considering the conditional access probability in (4), we have the b-th moment of the typical user when it is served by the i-th tier, given by

$$\begin{aligned} M_b^{(i)} &= \mathbb{E}_{R_i}\Big[\mathbb{P}(\iota(\mathrm{x}_0)=i \mid R_i) M_{b|(i),R_i}\Big] \\ &= \mathbb{E}_{R_i}\Bigg[\prod_{j\neq i} e^{-\lambda_j\pi(\hat{P}_{ij}\hat{B}_{ij})^{\delta}R_i^2}\prod_{\mathrm{x}\in\Phi_i}\frac{1}{(1+\theta R_i^{\alpha}R_{\mathrm{x}}^{-\alpha})^b} \\ &\quad\cdot\prod_{j\neq i}\prod_{\mathrm{x}\in\Phi_j}\frac{1}{(1+\theta\hat{P}_{ij}R_i^{\alpha}R_{\mathrm{x}}^{-\alpha})^b}\Bigg] \\ &\overset{(a)}{=} \mathbb{E}_{R_i}\Bigg[\prod_{j\neq i} e^{-\lambda_j\pi(\hat{P}_{ij}\hat{B}_{ij})^{\delta}R_i^2}\exp\Bigg(-2\lambda_i\pi \\ &\quad\cdot\int_{R_i}^{\infty}\Big[1-\frac{1}{(1+\theta R_i^{\alpha}x_i^{-\alpha})^b}\Big]x_i\mathrm{d}x_i\Bigg) \\ &\quad\cdot\prod_{j\neq i}\exp\Bigg(\int_{\hat{R}_j}^{\infty}-2\lambda_j\pi\Big[1-\frac{1}{\left(1+\theta\hat{P}_{ij}\left(\frac{R_i}{x_j}\right)^{\alpha}\right)^b}\Big]x_j\mathrm{d}x_j\Bigg)\Bigg] \\ &\overset{(b)}{=} \int_0^{\infty} 2\lambda_i\pi r_i e^{-\lambda_i\pi r_i^2} e^{-\sum\limits_{j\neq i}\lambda_j(\hat{P}_{ij}\hat{B}_{ij})^{\delta}\pi r_i^2} \\ &\quad\cdot\exp\Bigg(\int_{r_i}^{\infty}-2\lambda_i\pi\Big[1-\frac{1}{(1+\theta r_i^{\alpha}x_i^{-\alpha})^b}\Big]x_i\mathrm{d}x_i\Bigg) \\ &\quad\cdot\prod_{j\neq i}\exp\Bigg(\int_{\hat{r}_j}^{\infty}-2\lambda_j\pi\Big[1-\frac{1}{\left(1+\theta\hat{P}_{ij}\left(\frac{r_i}{x_j}\right)^{\alpha}\right)^b}\Big]x_j\mathrm{d}x_j\Bigg)\mathrm{d}r_i \\ &\overset{(c)}{=} \int_0^{\infty} e^{-z(1+\sum\limits_{j\neq i}\hat{\lambda}_{ij}(\hat{P}_{ij}\hat{B}_{ij})^{\delta})}\exp\Bigg(-2z\int_0^1\Big(1 \\ &\quad-\frac{1}{(1+\theta u_i^{\alpha})^b}\Big)u_i^{-3}\mathrm{d}u_i\Bigg)\prod_{j\neq i}\exp\Bigg(-2z \\ &\quad\cdot\int_0^{(\hat{P}_{ij}\hat{B}_{ij})^{-\frac{1}{\alpha}}}\Big(1-\frac{1}{(1+\theta\hat{P}_{ij}u_j^{\alpha})^b}\Big)u_j^{-3}\mathrm{d}u_j\Bigg)\mathrm{d}z \\ &\overset{(d)}{=} \int_0^{\infty} e^{-z}e^{-z\sum\limits_{j\neq i}\hat{\lambda}_{ij}(\hat{P}_{ij}\hat{B}_{ij})^{\delta}}\exp\Bigg(-z\int_1^{\infty}\Big(1 \\ &\quad-\frac{1}{(1+\theta t_i^{-\alpha/2})^b}\Big)\mathrm{d}t_i\Bigg)\prod_{j\neq i}\exp\Bigg(-z(\hat{P}_{ij}\hat{B}_{ij})^{\delta} \\ &\quad\cdot\int_1^{\infty}\Big(1-\frac{1}{(1+\theta\hat{B}_{ij}^{-1}t_j^{-\alpha/2})^b}\Big)\mathrm{d}t_j\Bigg)\mathrm{d}z, \end{aligned} \tag{51}$$

where (a) is by the PGFL of the PPP [26, Chap. 4], (b) is by averaging over R_i; (c) is by using the variable substitution $r_i/x_i = u_i$, $r_i/x_j = u_j$ and $\lambda_i\pi r_i^2 = z$, and (d) is by using the variable substitution $u_j = t_j(\hat{P}_{ij}\hat{B}_{ij})^{-\frac{1}{\alpha}}$.

By using the identity

$${}_2F_1(b,-\delta;1-\delta;-\theta) \equiv 1+\int_1^{\infty}\Big(1-\frac{1}{(1+\theta s^{-1/\delta})^b}\Big)\mathrm{d}s, \tag{52}$$

we obtain

$$M_b^{(i)} = \frac{1}{\sum\limits_j \hat{\lambda}_{ij}(\hat{P}_{ij}\hat{B}_{ij})^{\delta}\ {}_2F_1(b,-\delta;1-\delta;-\theta\hat{B}_{ij}^{-1})}. \tag{53}$$

Using

$$M_b^{(i)} = p_{\mathrm{a}}^{(i)}\cdot M_{b|(i)}, \tag{54}$$

and (48), we obtain (6). ■

B. Proof of Theorem 2

Proof: The b-th moment of the conditional success probability of the i-th tier is

$$\begin{aligned} &M_b^{(i)} \\ &= \mathbb{E}_{R_i}\Big[\mathbb{P}(\iota(\mathrm{x}_0)=i \mid R_i)M_{b|(i),R_i}\Big] \\ &= \mathbb{E}_{R_i}\Bigg[\prod_{j\neq i} e^{-\lambda_j\pi(\hat{P}_{ij}\hat{B}_{ij})^{\delta}R_i^2}\prod_{\mathrm{x}\in\Phi_i}\Big(\frac{p_i}{1+\theta R_i^{\alpha}R_{\mathrm{x}}^{-\alpha}}+1-p_i\Big)^b \end{aligned}$$

$$\cdot\prod_{j\neq i}\prod_{\mathrm{x}\in\Phi_j}\Big(\frac{p_j}{1+\theta\hat{P}_{ij}R_i^\alpha R_{\mathrm{x}}^{-\alpha}}+1-p_j\Big)^b\Big]$$
$$\stackrel{(a)}{=}\mathbb{E}_{R_i}\Big[\prod_{j\neq i}e^{-\lambda_j\pi(\hat{P}_{ij}\hat{B}_{ij})^\delta R_i^2}\exp\Big(\int_{R_i}^{\infty}-2\lambda_i\pi\Big[1-\Big(1 -\frac{p_i\theta R_i^\alpha x_i^{-\alpha}}{1+\theta R_i^\alpha x_i^{-\alpha}}\Big)^b\Big]x_i\mathrm{d}x_i\Big)\prod_{j\neq i}\exp\Big(\int_{\hat{R}_j}^{\infty}-2\lambda_j\pi \cdot\Big[1-\Big(\frac{p_j\theta\hat{P}_{ij}R_i^\alpha x_j^{-\alpha}}{1+\theta\hat{P}_{ij}R_i^\alpha x_j^{-\alpha}}\Big)^b\Big]x_j\mathrm{d}x_j\Big)\Big]$$
$$\stackrel{(b)}{=}\int_0^\infty 2\lambda_i\pi r_i e^{-\sum\limits_j\lambda_j(\hat{P}_{ij}\hat{B}_{ij})^\delta\pi r_i^2}\exp\Big(\int_{r_i}^{\infty}-2\lambda_i\pi \cdot\Big[1-\Big(1-\frac{p_i\theta r_i^\alpha x_i^{-\alpha}}{1+\theta r_i^\alpha x_i^{-\alpha}}\Big)^b\Big]x_i\mathrm{d}x_i\Big)\prod_{j\neq i}\exp\Big(\int_{\hat{r}_j}^{\infty}-2\lambda_j \cdot\pi\Big[1-\Big(\frac{p_j\theta\hat{P}_{ij}r_i^\alpha x_j^{-\alpha}}{1+\theta\hat{P}_{ij}r_i^\alpha x_j^{-\alpha}}\Big)^b\Big]x_j\mathrm{d}x_j\Big)\mathrm{d}r_i$$
$$\stackrel{(c)}{=}\int_0^\infty e^{-z}e^{-z\sum\limits_{j\neq i}\hat{\lambda}_{ij}(\hat{P}_{ij}\hat{B}_{ij})^\delta}\exp\Big(-2z\int_0^1\Big(1-\Big(1 -\frac{p_i\theta u_i^\alpha}{1+\theta u_i^\alpha}\Big)^b\Big)u_i^{-3}\mathrm{d}u_i\Big)\prod_{j\neq i}\exp\Big(-2z \cdot\int_0^{(\hat{P}_{ij}\hat{B}_{ij})^{-\frac{1}{\alpha}}}\hat{\lambda}_j\Big(1-\Big(1-\frac{p_j\theta\hat{P}_{ij}u_j^\alpha}{1+\theta\hat{P}_{ij}u_j^\alpha}\Big)^b\Big)u_j^{-3}\mathrm{d}u_j\Big)\mathrm{d}z$$
$$\stackrel{(d)}{=}\int_0^\infty e^{-z}e^{-z\sum\limits_{j\neq i}\hat{\lambda}_{ij}(\hat{P}_{ij}\hat{B}_{ij})^\delta}\exp\Big(-2z\int_0^1\Big(1-\Big(1 -\frac{p_i\theta u_i^\alpha}{1+\theta u_i^\alpha}\Big)^b\Big)u_i^{-3}\mathrm{d}u_i\Big)\prod_{j\neq i}\exp\Big(-z\hat{\lambda}_j(\hat{P}_{ij}\hat{B}_{ij})^\delta \cdot 2\int_0^1\Big(1-\Big(1-\frac{p_j\theta\hat{B}_{ij}^{-1}u_j^\alpha}{1+\theta\hat{B}_{ij}^{-1}u_j^\alpha}\Big)^b\Big)u_j^{-3}\mathrm{d}u_j\Big)\mathrm{d}z, \quad (55)$$

where (a) is by the PGFL of the PPP; (b) is by averaging over R_i; (c) is by using the variable substitution $r_i/x_i = u_i$, $r_i/x_j = u_j$ and $\lambda_i\pi r_i^2 = z$, and (d) is by using the variable substitution $u_j = u_j'(\hat{P}_{ij}\hat{B}_{ij})^{-\frac{1}{\alpha}}$.

Then from [11, Thm. 3], there is

$$\int_0^1\Big(1-\Big(1-\frac{p\theta r^\alpha}{1+\theta r^\alpha}\Big)^b\Big)r^{-3}\mathrm{d}r \equiv\sum_{k=1}^{\infty}\binom{b}{k}\frac{-(-p\theta)^k}{k\alpha-2}\,{}_2F_1(k,k-\delta;k-\delta+1;-\theta). \quad (56)$$

Hence,

$$M_b^{(i)}=\Big[\sum_j\hat{\lambda}_j(\hat{P}_{ij}\hat{B}_{ij})^\delta\Big(1-\sum_{k=1}^{\infty}\binom{b}{k}(-p_j\theta\hat{B}_{ij}^{-1})^k \cdot\frac{\delta}{k-\delta}\,{}_2F_1(k,k-\delta;k-\delta+1;-\theta\hat{B}_{ij}^{-1})\Big)\Big]^{-1}. \quad (57)$$

■

References

[1] A. Ghosh et al., "Heterogeneous cellular networks: From theory to practice," *IEEE Commun. Mag.*, vol. 50, no. 6, pp. 54–64, Jun. 2012.

[2] B. Błaszczyszyn, M. Haenggi, P. Keeler, and S. Mukherjee, *Stochastic Geometry Analysis of Cellular Networks*, Cambridge University Press, 2018.

[3] J. G. Andrews, F. B. Baccelli and R. K. Ganti, "A tractable approach to coverage and rate in cellular networks," *IEEE Trans. Commun.*, vol. 59, no. 11, pp. 3122–3134, Nov. 2011.

[4] H. S. Jo, Y. J. Sang, P. Xia and J. G. Andrews, "Heterogeneous cellular networks with flexible cell association: A comprehensive downlink SINR analysis," *IEEE Trans. Wireless Commun.*, vol. 11, no. 10, pp. 3484–3495, Oct. 2012.

[5] G. Nigam, P. Minero, and M. Haenggi, "Coordinated multipoint joint transmission in heterogeneous networks," *IEEE Trans. Commun.*, vol. 62, no. 11, pp. 4134–4146, Oct. 2014.

[6] H. S. Dhillon, R. K. Ganti, F. B. Baccelli and J. G. Andrews, "Modeling and analysis of K-tier downlink heterogeneous cellular networks," *IEEE J. Sel. Areas Commun.*, vol. 30, no. 3, pp. 550–560, Apr. 2012.

[7] S. Mukherjee, "Distribution of downlink SINR in heterogeneous cellular networks," *IEEE J. Sel. Areas Commun.*, vol. 30, no. 3, pp. 575–585, Apr. 2012.

[8] H. P. Keeler, B. Błaszczyszyn and M. K. Karray, "SINR-based k-coverage probability in cellular networks with arbitrary shadowing," *Proc. IEEE ISIT, 2013*, pp. 1167–1171.

[9] B. Błaszczyszyn and H. P. Keeler, "Studying the SINR process of the typical user in Poisson networks by using its factorial moment measures," *IEEE Trans. Inf. Theory*, vol. 61, no. 12, pp. 6774–6794, Dec. 2015.

[10] X. Zhang and M. Haenggi, "The performance of successive interference cancellation in random wireless networks," *IEEE Trans. Inf. Theory*, vol. 60, no. 10, pp. 6368–6388, Oct. 2014.

[11] M. Haenggi, "The meta distribution of the SIR in Poisson bipolar and cellular networks," *IEEE Trans. Wireless Commun.*, vol. 15, no. 44, pp. 2577–2589, Apr. 2016.

[12] M. Haenggi, "The mean interference-to-signal ratio and its key role in cellular and amorphous networks," *IEEE Wireless Commun. Lett.*, vol. 3, pp. 597–600, Dec. 2014.

[13] N. Deng, W. Zhou and M. Haenggi, "Heterogeneous cellular network models with dependence," *IEEE J. Sel. Areas Commun.*, vol. 33, no. 10, pp. 2167–2181, Oct. 2015.

[14] H. Wei, N. Deng, W. Zhou and M. Haenggi, "Approximate SIR analysis in general heterogeneous cellular networks," *IEEE Trans. Commun.*, vol. 64, no. 3, pp. 1259–1273, Mar. 2016.

[15] M. Salehi, A. Mohammadi, and M. Haenggi, "Analysis of D2D underlaid cellular networks: SIR meta distribution and mean local delay," *IEEE Trans. Commun.*, vol. 65, no. 7, pp. 2904–2916, Jul. 2017.

[16] Y. Wang, M. Haenggi and Z. Tan, "The meta distribution of the SIR for cellular networks with power control," *IEEE Trans. Commun.*, vol. 66, no. 4, pp. 1745–1757, Apr. 2018.

[17] Y. Wang, Q. Cui, M. Haenggi and Z. Tan, "On the SIR meta distribution for Poisson networks with interference cancellation," *IEEE Wireless Commun. Lett.*, vol. 7, no. 1, pp. 26–29, Feb. 2018.

[18] N. Deng and M. Haenggi, "A fine-grained analysis of millimeter-wave device-to-device networks," *IEEE Trans. Commun.*, vol. 65, no. 11, pp. 4940–4954, Nov. 2017.

[19] S. S. Kalamkar and M. Haenggi, "The spatial outage capacity of wireless networks," *IEEE Trans. Wireless Commun.*, vol. 17, no. 6, pp. 3709–3722, Jun. 2018.

[20] Q. Cui, X. Yu, Y. Wang and M. Haenggi, "The SIR meta distribution in Poisson cellular networks with base station cooperation," *IEEE Trans. Commun.*, vol. 66, no. 3, pp. 1234–1249, Mar. 2018.

[21] J. Gil-Pelaez, "Note on the inversion theorem," *Biometrika*, vol. 38, no. 3-4, pp. 481–482, 1951.

[22] M. Haenggi, "Efficient calculation of meta distributions and the performance of user percentiles", *IEEE Wireless Commun. Lett.*, accepted.

[23] A. Guo and M. Haenggi, "Asymptotic deployment gain: A simple approach to characterize the SINR distribution in general cellular networks," *IEEE Trans. Commun.*, vol. 64, no. 3, pp. 962–976, Mar. 2015.

[24] R. K. Ganti and M. Haenggi, "Asymptotics and approximation of the SIR distribution in general cellular networks," *IEEE Trans. Wireless Commun.*, vol. 15, no. 3, pp. 2130–2143, Mar. 2016.

[25] G. George, R. K. Mungara, A. Lozano, and M. Haenggi, "Ergodic spectral efficiency in MIMO cellular networks," *IEEE Trans. Wireless Commun.*, vol. 16, no. 5, pp. 2835–2849, May 2017.

[26] M. Haenggi, *Stochastic Geometry for Wireless Networks*. Cambridge University Press, 2012.

Yuanjie Wang received the B.S. degree of Communication Engineering and the Ph.D. degree of Communication and Information Systems from Beijing Jiaotong University (BJTU), Beijing, China, in 2010 and 2018, respective. He is currently with the National Computer Network Emergency Response Technical Team/Coordination Center of China (CNCERT/CC), Beijing, 100029, China. From January 2012 to November 2014, he was a research assistant in Nokia Solutions and Networks, Beijing. From November 2015 to December 2016, he was a visiting Ph.D. student at the University of Notre Dame, IN, USA, under the supervision of Professor Martin Haenggi. His research interests include modeling and analysis of cellular networks based on stochastic geometry, radio resource management for wireless networks and vehicular ad hoc networks.

Martin Haenggi (S'95-M'99-SM'04-F'14) received the Dipl.-Ing. (M.Sc.) and Dr.sc.techn. (Ph.D.) degrees in electrical engineering from the Swiss Federal Institute of Technology in Zurich (ETH) in 1995 and 1999, respectively. Currently he is the Freimann Professor of Electrical Engineering and a Concurrent Professor of Applied and Computational Mathematics and Statistics at the University of Notre Dame, Indiana, USA. In 2007-2008, he was a visiting professor at the University of California at San Diego, and in 2014-2015 he was an Invited Professor at EPFL, Switzerland.

He is a co-author of the monographs "Interference in Large Wireless Networks" (NOW Publishers, 2009) and "Stochastic Geometry Analysis of Cellular Networks" (Cambridge University Press, 2018) and the author of the textbook "Stochastic Geometry for Wireless Networks" (Cambridge, 2012), and he published 240 journal and conference papers, including 15 single-author journal articles. His scientific interests lie in networking and wireless communications, with an emphasis on cellular, amorphous, ad hoc (including D2D and M2M), cognitive, and vehicular networks.

He served as an Associate Editor of the Elsevier Journal of Ad Hoc Networks, the IEEE Transactions on Mobile Computing (TMC), the ACM Transactions on Sensor Networks, as a Guest Editor for the IEEE Journal on Selected Areas in Communications, the IEEE Transactions on Vehicular Technology, and the EURASIP Journal on Wireless Communications and Networking, as a Steering Committee member of the TMC, and as the Chair of the Executive Editorial Committee of the IEEE Transactions on Wireless Communications (TWC). From 2017 to 2018, he was the Editor-in-Chief of the TWC. He also served as a Distinguished Lecturer for the IEEE Circuits and Systems Society, as a TPC Co-chair of the Communication Theory Symposium of the 2012 IEEE International Conference on Communications (ICC'12), of the 2014 International Conference on Wireless Communications and Signal Processing (WCSP'14), and the 2016 International Symposium on Wireless Personal Multimedia Communications (WPMC'16). For both his M.Sc. and Ph.D. theses, he was awarded the ETH medal. He also received a CAREER award from the U.S. National Science Foundation in 2005 and three awards from the IEEE Communications Society, the 2010 Best Tutorial Paper award, the 2017 Stephen O. Rice Prize paper award, and the 2017 Best Survey paper award, and he is a 2017 and 2018 Clarivate Analytics Highly Cited Researcher.

Zhenhui Tan (SM'94) received the M.S. and Ph.D. degrees in Communications and Information Systems from Beijing Jiaotong University (BJTU), Beijing and Southeast University, Nanjing, China in 1982 and 1987, respectively. From 1990 to 1993, he was a visiting scholar at Mons Technology College, Belgium and at University of Waterloo, Canada. He has been with BJTU, where from 1993 to 1995 he was a director of Department of Communications and Signal Control Engineering in BJTU. From 1995 to 1998 he served as the Vice President of BJTU. From 1998 to 2008, he served as the President of BJTU. He was the chairman of the academic committee of BJTU.

His research interest include digital mobile communication networks, spread spectrum communications, broadband wireless access, adaptive filtering algorithms and beyond 4G systems. He published two books and more than 100 papers on communication and information areas.

Professor Tan was a member of the National Hi-Tech Project's Specialist Committee for three consecutive tenures, A member of the Evaluation Committee for Academic Degree Affairs of the State Council for two consecutive tenures, A member of Specialist Committee for Postdoctoral Degree Affairs, Director of electrical information science and engineering teaching guidance committee of Ministry of Education. Professor Tan was awarded titles of State Excellent Coming-Back From-Abroad Scholars and Experts of Outstanding Achievements from the State Council. Now he is a Fellow of the Chinese Institute of Communication (CIC) and the Chinese Institute of Railway (CIR), and also serves as the editor of the Chinese Journal of Electronics and the Journal of the China Railway Society.